

Some Studies on Pharmaceutical Eutectic – Nicotinamide - Benzamide System

Himanshu Shekhar¹ and Vishnu Kant^{2*}

Department of Chemistry, V.K.S.University, Ara-802301, India.

Corres.authors: ¹hshe2503@rediffmail.com, Mob.- 08877311180
²imvishnukant@gmail.com, Mob.: 9835061290

Abstract: The present investigation aims to measure the solid-liquid equilibria (SLE) of pharmaceutical active Nicotinamide (NA)-Benzamide (BZ) system and explore the thermodynamic and interfacial studies of the system. SLE data for the binary system was determined at atmospheric pressure by visually observing the melting points of a wide range of compositions maintaining accurate control of temperature. The phase diagram of the system shows the formation of simple eutectic at 0.391 mole fraction of BZ at the eutectic point, 105°C. Excess and mixing thermodynamic functions were calculated with the help of activity and activity coefficient values of components in binary mix. The excess functions predict the nature of molecular interaction and ordering in binary alloy whereas mixing functions suggest the nature of spontaneous and non-spontaneous mixing of the components. Interfacial morphology of the eutectic and non-eutectic alloys follows the Jackson's surface roughness () theory and predicts the faceted growth proceeds in the eutectic and non-eutectic alloys. The solid-liquid interfacial energy (σ), grain boundary energy (σ_{gb}) and the Gibb's Thomson coefficient (τ) of all the alloys are evaluated by using heat of fusion data. The driving force of nucleation during interfacial growth (ΔG_v), critical size or radius (r^*) and critical free energy of nucleation (ΔG^*) at different undercoolings have been determined.

Keywords: SLE, thermodynamic excess and mixing functions, interfacial energy, critical radius, critical free energy, roughness parameter.

Introduction

Nicotinamide, a derivative of the B vitamin niacin, is currently under trial for the prevention of insulin-dependent diabetes mellitus after success in the NOD mouse. However, the dose, route of administration, and formulation of nicotinamide^{1,2} given to humans is quite different from those used successfully in animals, and the plasma pharmacokinetics of oral nicotinamide in humans

with Enduramide was investigated^{3,4}. The AUC for standard nicotinamide was 1.7 times higher than that for Enduramide. It is water soluble vitamin. It has an anti inflammatory effect. It lacks the vasodilator, gastrointestinal, hepatic and hypolipemic action of niacin. As such nicotinamide has not been shown to produce the flushing, itching and burning sensations of the skin as is commonly seen when large doses of niacin are administered orally. It also represses antigen induced lymphocytic transformation and the

inhibition of 3'-5' cyclic AMP phosphodiesterase. It may prevent Type 2 diabetes mellitus⁵. Eutectic mixture formation between drugs and hydrophilic carriers was investigated⁶ recently to reduce the drug particle size, and increases the dissolution rate and thus changes the biopharmaceutical properties. Further it has been used mainly in two forms together with niacin both as food nutrient and a drug. It may be of benefit in patients with inflammatory acne vulgaris, including suppression of antigen induced-lymphocytic transformation and inhibition of 3' – 5' cycle AMP phosphodiesterase. These drugs were taken based on their poor solubility in water. However, interest in nicotinamide as a treatment for *M. tuberculosis* faded rapidly when one of the foremost research groups of the day reported antagonism between nicotinamide and isoniazid when they were used together as a 2-drug therapeutic regimen^{7,8}. In fact, a comprehensive review of nicotinamide's pharmaceutical effects came in light in 1991 as anti HIV agent⁹ and after that popularized vastly. In the present study Nicotinamide(NA)-Benzamide(BZ) drug system was selected for the solid-liquid equilibrium phase diagram, thermodynamic and interfacial investigations of eutectic and non-eutectic drug alloys soluble in water.

Experimental

Nicotinamide (Thomas Baker, Mumbai) and Benzamide (Rohini Mumbai, India) were directly taken for investigation. The melting point (experimental and literature value) of nicotinamide was found 128°C while for Benzamide was found 127°C and 125-127°C respectively. For measuring the solid-liquid equilibrium data of NA-BZ system, mixtures of different composition were made in glass test tubes by repeated heating and followed by chilling in ice and were determined by the thaw-melt method^{10,11}. The melting and thaw temperatures were determined in a Toshniwal melting point apparatus using a precision thermometer which could read correctly up to $\pm 0.1^\circ\text{C}$. The heater was regulated to give above 1°C increase in temperature in every five minutes.

Heat of fusion of materials was measured by the DTA method using NETZSCH Simultaneous Thermal Analyzer, STA 409 series unit. All the runs were carried out with heating rate $2^\circ\text{C}/\text{min}$, chart speed 10mm/min and chart sensitivity $100\mu\text{v}/10\text{mv}$. The sample weight was 5 mg for all estimation. Using benzoic acid was a standard substance, the heat of fusion of unknown compound was determined^{12,13} using the following equation:

$$\Delta H_x = \frac{\Delta H_s W_s A_x}{W_x A_s}$$

where H_x is the heat of fusion of unknown sample and H_s is the heat of fusion of standard substance. W and A are weight and peak area, respectively and suffices x and s indicate the corresponding quantities for the unknown and standard substances, respectively.

Result and Discussion

SLE Study

The SLE data of NA-BZ system determined by the thaw melt method, is reported (Table 1) in the form of temperature-composition curve in Fig.1. The system shows the formation of a simple eutectic. The melting point of NA (128°C) decreases on the addition of second component BZ (M.P., 127°C) and further attains minimum and then increases. Eutectic alloys E(0.391 mole fraction of BZ) are obtained at 105°C . At the eutectic temperature two phases namely a liquid phase L and two solid phases (S_1 and S_2) are in equilibrium and the system is invariant. In the region indicated by L a homogenous binary liquid solution exists while the two solid phases exists below the horizontal line. In the case, in region located on the left side of the diagram a binary liquid and solid NA exist while in a similar region located on the right side of the diagram a binary liquid and the second component of the system co-exist.

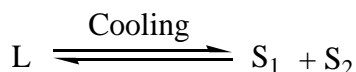
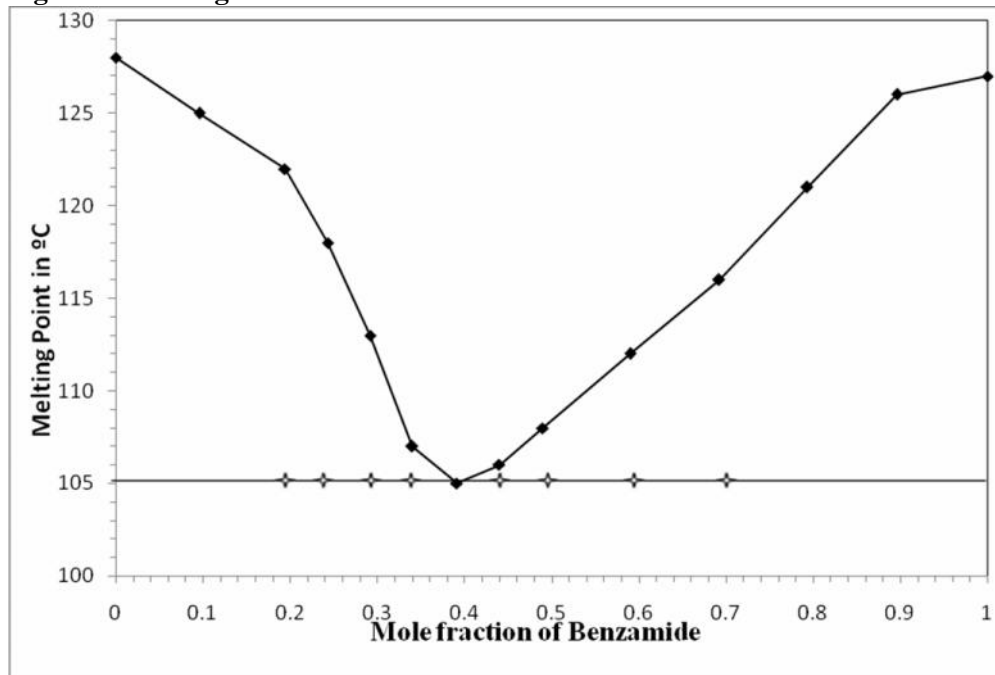


Table 1: Phase composition, melting temperature, values of entropy of fusion and entropy of fusion per unit volume (S_v), heat of fusion(UH), interfacial energy(γ), grain boundary energy(γ_{gb}), Gibbs-Thomson coefficient (γ) and roughness parameter(r)

Alloy	X_{BZ}	MP (°C)	S (J/mol)	$\times 10^2$ J/m	$\gamma_{gb} \times 10^2$ J/m	S_v (kJ/m ³ /K)	$\gamma \times 10^5$ Km		
A ₁	0.896	126	23518.4	58.943	7.090	3.894	7.524	514	1.463
A ₂	0.793	121	23734.7	60.240	7.246	4.004	7.735	540	1.431
A ₃	0.692	116	23946.8	61.560	7.404	4.116	7.952	568	1.400
A ₄	0.590	112	24161.0	62.756	7.548	4.234	8.181	596	1.372
A ₅	0.490	108	24371.0	63.966	7.694	4.356	8.415	626	1.345
A ₆	0.440	106	24476.0	64.580	7.768	4.419	8.537	641	1.331
E	0.391	105	24578.9	65.024	7.821	4.482	8.659	656	1.321
A ₇	0.340	107	24686.0	64.963	7.814	4.550	8.789	665	1.321
A ₈	0.292	113	24786.8	64.214	7.724	4.614	8.914	668	1.335
A ₉	0.243	118	24889.7	63.656	7.656	4.682	9.046	672	1.345
A ₁₀	0.194	122	24992.6	63.272	7.610	4.752	9.180	679	1.352
A ₁₁	0.096	125	25198.4	63.313	7.615	4.897	9.460	702	1.347
NA	0	128	25400	63.342	7.619	5.046	9.748	726	1.343
BZ	1	127	23300	58.250	7.006	3.789	7.319	494	1.480

Fig 1: Phase diagram of Nicotinamide and Benzamide



◆ Thaw temperature; ■ Melting temperature

Thermodynamic Study

The values of heats of fusion of eutectic and noneutectic alloys and are calculated by the mixture law. The value of heat of fusion of binary alloys A₁-A₁₁, E is reported in Table 1. The activity coefficient and activity of components for the systems under investigation has been calculated from the equation¹⁴ given below

$$- \ln x_i \gamma_i = \frac{\Delta H_i}{R} \left(\frac{1}{T_e} - \frac{1}{T_i} \right) \quad (1)$$

where γ_i is activity coefficient of the component i in the liquid phase respectively, H_i is the heat of fusion of component i at melting point T_i and R is the gas constant. T_e is the melting temperature of alloy. Using the values of activity and activity coefficient of the components in alloys mixing and excess thermodynamics functions have been computed.

Mixing Functions

In order to know the mixing characteristics of components in the alloy Integral molar free energy of mixing (G^M), molar entropy of mixing (S^M) and molar enthalpy of mixing (H^M) and partial thermodynamic mixing functions of the binary alloys were determined by using the following equations

$$G^M = RT (x_{NA} \ln a_{NA} + x_{BZ} \ln a_{BZ}) \quad (2)$$

$$S^M = -R (x_{NA} \ln x_{NA} + x_{BZ} \ln x_{BZ}) \quad (3)$$

$$H^M = RT (x_{NA} \ln \gamma_{NA} + x_{BZ} \ln \gamma_{BZ}) \quad (4)$$

$$G_i^{-M} = \mu_i^{-M} = RT \ln a_i \quad (5)$$

where G_i^{-M} (μ_i^{-M}) is the partial molar free energy of mixing of component i (mixing chemical potential) in binary mix. and γ_i and a_i is the activity coefficient and activity of component respectively. The positive value^{15,16} of molar free energy of mixing of alloys (Table 2) suggests that the mixing in all cases is non-spontaneous. The integral molar enthalpy of mixing value corresponds to the value of

excess integral molar free energy of the system favors the regularity in the binary solutions.

Excess Functions

In order to unfold the nature of the interactions between the components forming the eutectic, non-eutectic alloys and addition compound, the excess thermodynamic functions such as integral excess integral free energy (g^E), excess integral entropy (s^E) and excess integral enthalpy (h^E) were calculated using the following equations

$$g^E = RT (x_{NA} \ln \gamma_{NA} + x_{BZ} \ln \gamma_{BZ}) \quad (6)$$

$$s^E = -R \left(x_{NA} \ln \gamma_{NA} + x_{BZ} \ln \gamma_{BZ} + x_{NA} T \frac{\delta \ln \gamma_{NA}}{\delta T} + x_{BZ} T \frac{\delta \ln \gamma_{NA}}{\delta T} \right) \quad (7)$$

$$h^E = -RT^2 \left(x_{NA} \frac{\delta \ln \gamma_{NA}}{\delta T} + x_{BZ} \frac{\delta \ln \gamma_{BZ}}{\delta T} \right) \quad (8)$$

and excess chemical potential or excess partial free energy of mixing

$$g_i^{-E} = \mu_i^{-M} = RT \ln \gamma_i \quad (9)$$

The values of $\ln \gamma_i / T$ can be determined by the slope of liquidus curve near the alloys form in the phase diagram. The values of the excess thermodynamic functions are given in Table 3. The value of the excess free energy is a measure of the departure of the system from ideal behavior. The reported excess thermodynamic data substantiate the earlier conclusion of an appreciable interaction between the parent components during the formation of alloys. The negative value of excess free energy indicates the possibility of a stronger association between unlike molecules while the positive value in the present system suggests an association of weaker nature between unlike molecules and of stronger nature between like molecules. The maximum positive g^E value¹⁷ for all eutectic and non-eutectic alloys infers stronger interaction between like molecules in binary mix. The excess entropy is a measure of the change in configurational energy due to a change in potential energy and indicates an increase in randomness.

Table 2: Value of partial and integral mixing of gibbs free energy(UG^M), enthalpy(UY^{\wedge}) and entropy(US^{\wedge}) of NA-BZ system

Alloy	$UG_{NA}^{>M}$ J/mol	$UG_{BZ}^{>M}$ J/mol	UG^M J/mol	UY_{11}^{-M} J/mol	UH_{BZ}^{-M} J/mol	UY^{\wedge} J/mol	US_{NA}^{-M} J/mol/K	US_{BZ}^{-M} J/mol/K	US^{\wedge} J/mol/K
A ₁	3192.991	176.515	490.2287	7381.544	540.803	1252.240	18.818	0.913	2.775
A ₂	2861.023	-117.677	498.9141	4715.981	642.067	1485.367	13.095	1.928	4.240
A ₃	2556.762	-411.869	502.4695	3048.61	778.845	1477.932	9.791	3.061	5.134
A ₄	2332.192	-647.222	574.3377	1840.441	1041.672	1369.167	7.413	4.387	5.627
A ₅	2123.477	-882.576	650.5109	866.076	1377.056	1116.456	5.598	5.931	5.761
A ₆	2024.812	-1000.253	693.7837	433.495	1586.662	940.889	4.821	6.826	5.703
E	1976.86	-1059.091	789.8032	101.719	1892.047	801.737	4.123	7.807	5.564
A ₇	2073.68	-941.414	1048.548	-17.428	2466.891	827.240	3.454	8.969	5.330
A ₈	2386.817	-588.384	1518.058	158.049	3362.151	1093.647	2.871	10.234	5.021
A ₉	2675.248	-294.192	1953.674	271.573	4304.658	1251.613	2.314	11.762	4.610
A ₁₀	2925.147	-58.838	2346.254	328.222	5326.633	1297.914	1.793	13.634	4.090
A ₁₁	3124.3	117.677	2835.665	143.936	7871.945	885.825	0.839	19.483	2.629

Table 3: Value of partial and integral excess gibbs free energy(g^E), enthalpy(h^E) and entropy(s^E) of NA-BZ system

Alloy	g_{NA}^{-E} J/mol	g_{BZ}^{-E} J/mol	g^E J/mol	h_{NA}^{-E} J/mol	h_{BZ}^{-E} J/mol	h^E J/mol	S_{NA}^{-E} J/mol/K	S_{BZ}^{-E} J/mol/K	S^E J/mol/K
A ₁	7381.544	540.802	1252.240	483675.813	35789.157	82369.370	1193.720	88.342	203.301
A ₂	4715.981	642.067	1485.367	99298.754	9250.620	27890.580	240.0578	21.849	67.018
A ₃	3048.610	778.845	1477.932	28926.302	879.915	9518.202	66.524	0.260	20.669
A ₄	1840.441	1041.672	1369.167	54852.558	32468.727	41646.100	137.694	81.629	104.615
A ₅	866.076	1377.056	1116.456	21928.178	25959.941	23903.740	55.281	64.522	59.809
A ₆	433.495	1586.662	940.889	38576.675	58124.860	47177.880	100.642	149.177	121.997
E	101.719	1892.047	801.737	169663.641	280520.352	213008.600	448.576	737.112	561.394
A ₇	-17.428	2466.891	827.240	-1207.268	23662.362	7248.407	-3.131	55.778	16.898
A ₈	158.049	3362.151	1093.647	-7903.492	19123.039	-11.745	-20.885	40.831	-2.864
A ₉	271.573	4304.658	1251.613	-8609.344	29006.693	531.353	-22.713	63.176	-1.842
A ₁₀	328.222	5326.633	1297.914	6788.383	110431.119	26895.070	16.355	266.087	64.803
A ₁₁	143.936	7871.945	885.825	18304.785	388253.392	53819.850	45.630	955.732	133.000

Gibbs-Duhem Equation

Further the partial molar quantity, activity and activity coefficient can also be determined by using Gibbs-Duhem equation¹⁸

$$\sum x_i dz_i^{-M} = 0 \tag{10}$$

$$\text{or } x_{NA} dH_{NA}^{-M} + x_{BZ} dH_{BZ}^{-M} = 0 \tag{11}$$

$$\text{or } dH_{NA}^{-M} = \frac{x_{BZ}}{x_{NA}} dH_{BZ}^{-M} \tag{12}$$

$$\text{or } [H_{NA}^{-M}]_{x_{NA}=y} = \int_{x_{NA}=y}^{x_{NA}=1} \frac{x_{BZ}}{x_{NA}} dH_{BZ}^{-M} \tag{13}$$

Using equation (14) a graph (Fig. 2) between H_{BZ}^{-M} and x_{BZ}/x_{NA} gives the solution of the partial molar heat of mixing of a constituent NA in NA/BZ alloy and plot between x_{BZ}/x_{NA} vs $\ln a_{NA}$ determines the value of activity (Fig. 3) of component NA in binary alloys.

Fig 2: Graphical solution of partial molar enthalpy of mixing in binary mix

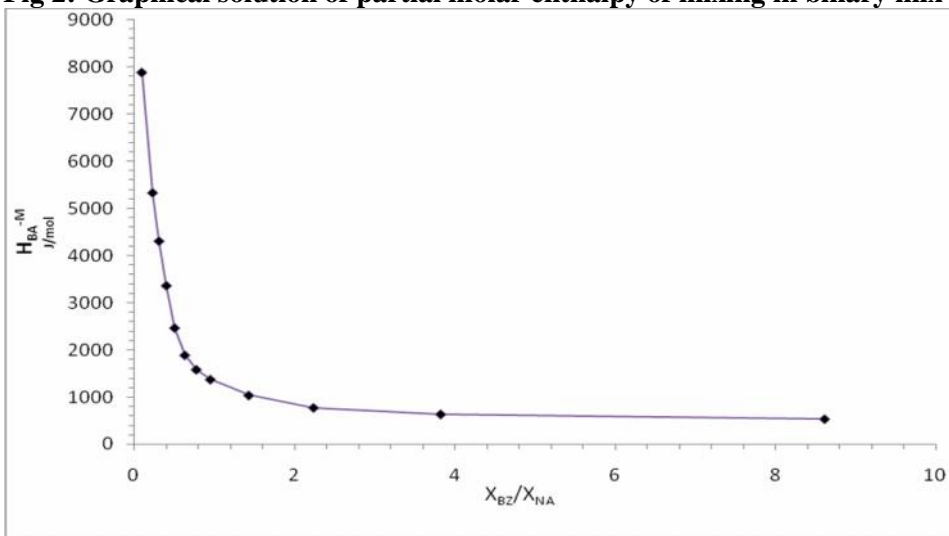
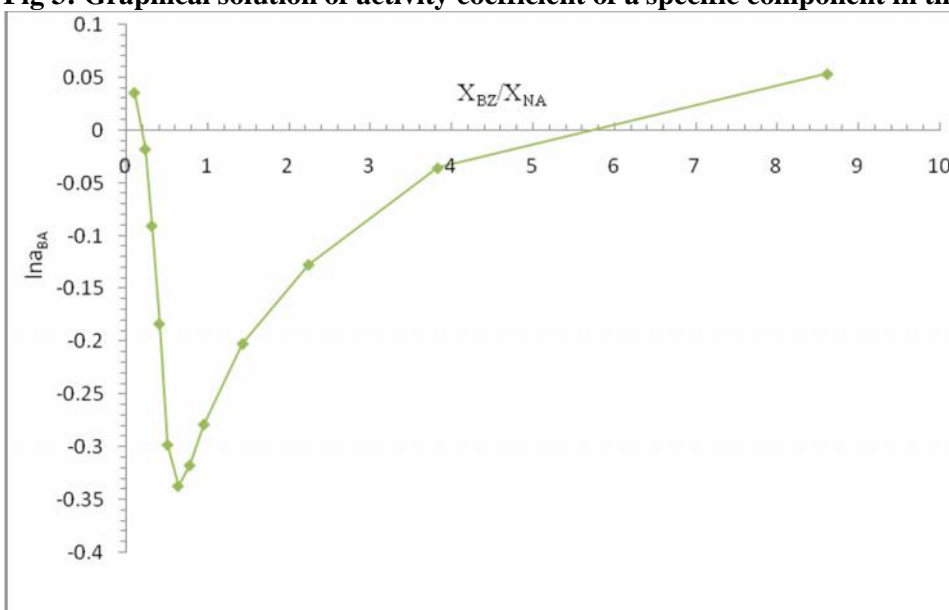


Fig 3: Graphical solution of activity coefficient of a specific component in the binary mix



Interfacial Investigation

Interface Morphology

The science of growth has been developed on the foundation of thermodynamics, kinetics, fluid dynamics, crystal structures and interfacial sciences. The solid-liquid interface morphology can be predicted from the value of the entropy of fusion. According to Hunt and Jackson¹⁹, the type of growth from a binary melt depends upon a factor α , defined as:

$$\alpha = \xi \frac{\Delta H}{RT} = \xi \frac{\Delta S}{R} \quad (14)$$

where ξ is a crystallographic factor depending upon the geometry of the molecules and has a value less than or equal to one. $\Delta S/R$ (also known as Jackson's roughness parameter) is the entropy of fusion (dimensionless) and R is the gas constant. When α is less than two the solid-liquid interface is atomically rough and exhibits non-faceted growth. The value of Jackson's roughness parameter ($\Delta S/R$) is given in Table 1. For the entire alloy the α value was found greater than 2 which indicate the faceted²⁵ growth proceeds in all the cases.

The Solid-Liquid Interfacial Energy (σ)

It has been found that an experimentally observed value of interfacial energy ' σ ' keeps a variation of 50-100% from one worker to other. However, Singh and Glickman²⁰ were calculated the solid-liquid interfacial energy (σ) from melting enthalpy change and values obtained are found in good agreement with the experimental values. Turnbull empirical relationship²¹ between the interfacial energy and enthalpy change provides the clue to determine the interfacial energy value of alloy and is expressed as:

$$\sigma = \frac{C\Delta H}{(N)^{1/3}(V_m)^{2/3}} \quad (15)$$

where the coefficient C lies between 0.33 to 0.35 for nonmetallic system, V_m is molar volume and N is the Avogadro's constant. The value of the solid-liquid interfacial energy of nicotinamide and benzamide was found to be 5.046×10^{-02} and $3.789 \times 10^{-02} \text{ J m}^{-2}$ respectively and α value of alloys was given in Table 1.

The Effective Entropy Change (ΔS_v)

It is obvious that the effective entropy change and the volume fraction of phases in the alloy are inter-related to decide the interface morphology during solidification and the volume fraction of the two phases depends on the ratio of effective entropy change of the phases. The entropy of fusion ($\Delta S = \Delta H/T$) value (Table 1) of alloys is calculated by heat of fusion values of the materials. The effective entropy change per unit volume (ΔS_v) is given by

$$\Delta S_v = \frac{\Delta H}{T} \cdot \frac{1}{V_m} \quad (16)$$

where ΔH is the enthalpy change, T is the melting temperature and V_m is the molar volume of solid phase. The entropy of fusion per unit volume (ΔS_v) for NA and BZ was found 726 and 494 $\text{kJ K}^{-1} \text{m}^{-3}$ respectively. Values of ΔS_v for alloys are reported in Table 1.

The Driving Force of Nucleation (ΔG_v)

During growth of crystalline solid there is change in enthalpy, entropy and specific volume and non-equilibrium leads to Gibbs' energy. Thermodynamically metastable phase occurs in a supersaturated or super-cooled liquid. The driving force for liquid-solid transition is the difference in Gibbs' energy between the two phases. The theories of solidification process in past have been discussed on the basis of diffusion model, kinetic characteristics of nucleation and on thermodynamic features. The lateral motion of rudimentary steps in liquid advances stepwise/ non-uniform surface at low driving force while continuous and uniform surface advances at sufficiently high driving force. The driving force of nucleation from liquid to solid during solidification (ΔG_v) can be determined at different undercoolings (ΔT) by using the following equation²²

$$\Delta G_v = \Delta S_v \Delta T \quad (17)$$

It is opposed by the increase in surface free energy due to creation of a new solid-liquid interface. By assuming that solid phase nucleates as small spherical cluster of radius arising due to random motion of atoms within liquid. The value of ΔG_v for alloys and pure components are shown in the Table 4.

Table 4: Value of free energy change (UG_v) during solidification for NA-BZ system at different undercoolings(UT)

Alloy	UG _v (kJ/m ³)					
	1.0	1.5	2.0	2.5	3.0	3.5
A ₁	0.514	0.771	1.028	1.286	1.543	1.800
A ₂	0.540	0.811	1.081	1.351	1.621	1.891
A ₃	0.568	0.852	1.136	1.420	1.704	1.988
A ₄	0.596	0.894	1.192	1.490	1.788	2.086
A ₅	0.626	0.939	1.252	1.564	1.877	2.190
A ₆	0.641	0.962	1.283	1.603	1.924	2.245
E	0.656	0.983	1.311	1.639	1.967	2.294
A ₇	0.665	0.998	1.331	1.663	1.996	2.329
A ₈	0.668	1.002	1.336	1.669	2.003	2.337
A ₉	0.672	1.009	1.345	1.681	2.017	2.354
A ₁₀	0.679	1.019	1.358	1.698	2.037	2.377
A ₁₁	0.702	1.053	1.404	1.755	2.106	2.457
NA	0.726	1.089	1.452	1.815	2.178	2.541
BZ	0.494	0.742	0.989	1.236	1.483	1.730

The Critical Radius (r*)

During liquid-solid transformation embryos are rapidly dispersed in unsaturated liquid and on undercooling liquid becomes saturated and provide embryo of a critical size with radius r* for nucleation which can be expressed by the Chadwick relation²³

$$r^* = \frac{2\sigma}{\Delta G_v} = \frac{2\sigma T}{\Delta H_v \Delta T} \quad (18)$$

where σ is the interfacial energy and H_v is the enthalpy of fusion of the compound per unit volume, respectively. The critical size of the nucleus for the components and alloys was calculated at different undercoolings and values are presented in Table 5. It can be inferred from table that the size of the critical nucleus decreases with increase in the undercooling of the melt. The existence of embryo and a range of embryo size can be expected in the liquid at any temperature.

Critical Free Energy of Nucleation (UG*)

To form critical nucleus, it requires a localized critical free energy of nucleation (ΔG^*) which is evaluated²⁴ as

$$\Delta G^* = \frac{16 \pi \sigma^3}{3 \Delta G_v^2} \quad (19)$$

The value of ΔG^* for alloys and pure components has been found in the range of 10^{15} to 10^{16} J at different undercoolings, and has been reported in Table 6.

Gibbs-Thomson Coefficient (τ)

For a planar grain boundary on planar solid-liquid interface the Gibbs-Thomson coefficient (τ) for the system can be calculated by the Gibbs-Thomson equation is expressed as

$$\tau = r\Delta T = \frac{TV_m\sigma}{\Delta H} = \frac{\sigma}{\Delta S_v} \quad (20)$$

where τ is the Gibbs-Thomson coefficient, T is the dispersion in equilibrium temperature and, r is the radius of grooves of interface. The theoretical basis of determination of τ was made for equal thermal conductivities of solid and liquid phases for some transparent materials. It was also determined by the help of Gunduz and Hunt numerical method²⁵ for materials having known grain boundary shape, temperature gradient in solid and the ratio of thermal conductivity of the equilibrated liquid phases to solid phase ($R = K_L/K_S$).The Gibbs-Thomson coefficient for NA, BZ and their alloys are found in the range of 1.321 – 1.480×10^{-05} Km and is reported in Table 1.

Interfacial Grain Boundary Energy (τ_{gb})

Grain boundary is the internal surface which can be understood in a very similar way to nucleation on surfaces in liquid-solid transformation. In past, a numerical method²⁶ is applied to observe the interfacial grain boundary energy (τ_{gb}) without applying the temperature gradient for the grain boundary groove shape. For isotropic interface there is no difference in the value of interfacial tension and interfacial energy. A considerable force is employed at the grain boundary groove in anisotropic interface. The

grain boundary energy can be obtained by the equation:

$$\sigma_{gb} = 2\sigma \cos \theta \quad (21)$$

where θ is equilibrium contact angle precipitates at solid-liquid interface of grain boundary. The grain boundary energy could be twice the solid-liquid

interfacial energy in the case where the contact angle tends to zero. The value of σ_{gb} for solid NA and BZ was found to be 9.748×10^{-2} and $7.319 \times 10^{-2} \text{Jm}^{-2}$ respectively and the value for all alloys is given in Table 1.

Table 5: Critical size of nucleus (r^*) at different undercoolings(UT)

Alloy	$r^*(\text{m}) \times 10^7$					
	1.0	1.5	2.0	2.5	3.0	3.5
A ₁	1.51	2.27	3.03	3.79	4.54	5.30
A ₂	1.48	2.22	2.96	3.70	4.45	5.19
A ₃	1.45	2.17	2.90	3.62	4.35	5.07
A ₄	1.42	2.13	2.84	3.55	4.26	4.97
A ₅	1.39	2.09	2.78	3.48	4.18	4.87
A ₆	1.38	2.07	2.76	3.44	4.13	4.82
E	1.37	2.05	2.73	3.42	4.10	4.79
A ₇	1.37	2.05	2.73	3.42	4.10	4.79
A ₈	1.38	2.07	2.76	3.46	4.15	4.84
A ₉	1.39	2.09	2.79	3.48	4.18	4.87
A ₁₀	1.40	2.10	2.80	3.50	4.20	4.90
A ₁₁	1.39	2.09	2.79	3.49	4.18	4.88
NA	1.39	2.08	2.78	3.47	4.17	4.86
BZ	1.53	2.30	3.06	3.83	4.60	5.36

Table 6: Value of critical free energy of nucleation (UG^*) for alloys of NA-BZ system at different undercoolings(UT)

Alloy	$UG^*(\text{J}) \times 10^{16}$					
	1.0	1.5	2.0	2.5	3.0	3.5
A ₁	37.4	16.6	9.36	5.99	4.16	3.06
A ₂	36.8	16.4	9.21	5.90	4.09	3.01
A ₃	36.2	16.1	9.06	5.80	4.03	2.96
A ₄	35.8	15.9	8.95	5.73	3.98	2.92
A ₅	35.4	15.7	8.85	5.66	3.93	2.89
A ₆	35.2	15.6	8.79	5.63	3.91	2.87
E	35.1	15.6	8.78	5.62	3.90	2.87
A ₇	35.7	15.8	8.91	5.70	3.96	2.91
A ₈	36.9	16.4	9.23	5.91	4.10	3.02
A ₉	38.1	16.9	9.51	6.09	4.23	3.11
A ₁₀	39.0	17.3	9.75	6.24	4.33	3.18
A ₁₁	39.9	17.7	9.98	6.39	4.44	3.26
NA	40.8	18.2	1.02	6.54	4.54	3.33
BZ	37.3	16.6	9.32	5.97	4.14	3.04

Conclusion

The solid-liquid equilibrium phase diagram of NA-BZ system shows the formation of simple eutectic alloy. The activity and activity coefficient values are very useful in computing thermodynamic mixing and excess functions. Thermodynamic excess and mixing functions g^E and ΔG^M values for eutectic and non-eutectic

alloys are being found positive which suggest the stronger association between like molecules and there is non-spontaneous mixing in all the binary alloys.

Acknowledgement

Thanks are due to the Head Department of Chemistry, V K S University Ara 802301, India for providing research facilities.

References

- Miedzobrodzki J., Lach G., Jaworek R. and Panz T., Effect of Nicotinamide and Its Two Derivatives on The Generation of Reactive Oxygen Species in Human Monocytes Cooperating with Platelets, *Acta Poloniae Pharmaceutica-Drug Research*, 2010, 67(5), 487-494.
- Goodman A., Gilman A., "The Pharmacological Basis of Therapeutics", McGraw Hill, 11th ed., 2006, 955-957.
- Yamaguchi T., Matsumura Y., Ishii T., Tokuoka Y., Kurita K., Synthesis of nicotinamide derivatives having a hydroxyl-substituted benzene ring and the influence of their structures on the apoptosis-inducing activity against leukemia cells, *Drug Development Research*, 2011, 72(3), 289-297.
- Jacobson E. L., Dame A. J., Pyrek J. S., Jobson M. K., Evaluating the role of niacin in human carcinogenesis, *Biochemie*, 1995, 77, 394.
- LeClaire R. D., Kell W., Bavari S, Smith T. J., Hunt R. E., Protective effects of niacinamide in staphylococcal enterotoxin-B-induced toxicity, *Toxicology*, 1996, 107, 69-81.
- Terauchi H., Tanitame A., Tada K., Nakamura K., Seto Y. and Nishikawa Y., Nicotinamide derivatives as a New Class and Structure-Activity Relationships of N-Substituted 2-(Benzhydryl- and benzylsulfinyl)nicotinamide, *J. Med. Chem.*, 1997, 40(3), 313-321.
- Jordahl C., Desprez R., Muchenheim C., Deuschle K. and McDermott W., Ineffectiveness of niacinamide and isoniazide in treatment of pulmonary tuberculosis, *Am. Rev. Respir. Dis.*, 1961, 83, 899-901.
- Girgis A. S., Hosni H. M. and Barsoum F. F., Novel synthesis of nicotinamide derivatives of cytotoxic properties, *Bioinorganic and Medical Chemistry*, 2006, 14(13), 4466-4476.
- Murray Michael F., Nicotinamide: An Oral Antimicrobial Agent with Activity against Both Mycobacterium tuberculosis and Human Immunodeficiency Virus, *Clinical Infectious Diseases*, 2003, 36, 453-460.
- Dwivedy Y., Kant S., Rai U. S. and Rai R. N., Synthesis, Physicochemical and Optical Characterization of Novel Fluorescing Complex:o-Phenylenediamine-Benzoin, *Journal of Fluorescence*, 2011, 21, 1255-1263.
- Sharama B. L., Tandon S. and Gupta S., Characteristics of the binary faceted eutectic; benzoic Acid-Salicylic Acid system, *Cryst. Res. Technol*, 2009, 44, 258-268.
- Krajewska-Cizio A., Phase diagram in the binary systems of N-isopropylcarbazole with 2,4,7-trinitrofluoren-9-one and carbazole, *Thermochemica Acta*, 1990, 158, 317-325.
- Sangster J., Phase diagram and thermodynamic properties of organic systems based on 1,2- 1,3- 1,4-Diaminobenzene, *J. Phy. Chem. Ref. Data*, 1994, 23, 295-317.
- Shekhar H. and Salim S. S., Molecular interactions and stability in binary organic alloys, *J. Nat. Acad. Sci Letter*, 2011, 34, 117-125.
- Wisniak J. and Tamir A., Mixing and Excess Thermodynamic Properties (a literature source book), *Phys. Sci. Data 1*, Elsevier, New York, 1978.
- Nieto R., Gonozalez M. C., Herrero F., Thermodynamics of mixtures, functions of mixing and excess functions, *American Journal of Physics*, 1999, 67, 1096-1099.
- Agrwal T., Gupta P., Das S. S., Gupta A. and Singh N. B., Phase equilibria crystallization and microstructural studies of Naphthalen-2-ol + 1,3-Dinitrobenzene, *J. Chem. Engg. Data*, 2010, 55, 4206-4210.
- Shamsuddin M., Singh S. B. and Nasar A., Thermodynamic investigations of liquid gallium-cadmium alloys, *Thermochemica Acta*, 1998, 316, 11-19.

19. Hunt J. D., Jackson K. A., Trans. Metall. Soc. AIME, 1966, 236, 843.
20. Singh N. B., Glicksman M. E., Determination of the mean solid-liquid interface energy of pivalic acid, J. Cryst. Growth, 1989, 98, 573-580.
21. Turnbull D., Formation of crystal nuclei in liquid metals, J. Chem. Phys., 1950, 18, 768.
22. Hunt J. D. and Lu S. Z., Hand Book of Crystal Growth Ed. DTJ Hurle, Elsevier, Amsterdam, 1994, 112
23. Chadwick G. A., Metallography of Phase Transformation, Butterworths, London, 1972, 61.
24. Wilcox W. R., The relation between classical nucleation theory and the solubility of small particles, Journal of crystal growth, 1974, 26, 153-154.
25. Gunduz M., Hunt J. D., Acta Metall., 1989, 37, 1839.
26. Akbulut S., Ocak Y., Keslioglu K., Marasli N., Determination of interfacial energies in the aminomethyl propanediol-neopentylglycol organic alloy, Applied Surface Science, 2009, 255, 3594-3599.
